Proceedings of the 9th World Congress on Electrical Engineering and Computer Systems and Sciences (EECSS'23)
Brunel University, London, United Kingdom – August 03-05, 2023
Paper No. ICBES 121
DOI: 10.11159/icbes223.121

Qualitative Assessment of Myocardial Gray Zone in LGE-CMR Imaging

Maria Narciso[1,2], António Ferreira[3], Pedro Vieira[1,2]
[1]Physics Department, NOVA School of Science and Technology
2829-516, Caparica, Portugal
m.narciso@campus.fct.unl.pt
[2]Bee2Fire SA
2200-062, Abrantes, Portugal
[3]Centro Hospitalar de Lisboa Ocidental
2790-134, Carnaxide, Portugal

Abstract **-** Our ongoing research is centered on developing patient-customized computational heart models to study arrhythmia mechanisms and risk assessment. The long-term goal is improving patient selection for a cardio-defibrillator implantation. This device is necessary when the normal pattern of electrical propagation is disrupted in a way that causes the heart rhythm to be so disorganized that the pumping function is compromised. This type of arrhythmia is named fibrillation and can only be stopped by an immediate intervention, if not, the brain irrigation is intercepted resulting in sudden cardiac death. Our approach to assessing if an individual is at risk of going through this event is to study the electrical propagation on their own heart using a parallel model. In the present article, we propose a novel method to add a qualitative rating to scarred myocardium. A left ventricle computational model is built, based on an anonymized cardiac magnetic resonance data set with visible scars. The scarred areas are identified and divided into the scar's core, made of dead cells where the conductivity is null, and the heterogeneous or gray zones where different levels of fibrosis coexist, forming both viable and nonviable paths for the depolarization wave. After this major segmentation, the gray zones are split into subsets and the conductivities are computed according to the intensity of the pixels. The number of subsets can be set between two and five. In this work, we are considering two scenarios: with one gray zone level and two. Resulting in two possible patterns the depolarization signal can obey. Electrophysiological simulations are performed for each scenario using the open-source software CHASTE (Cancer, Heart, and Soft Tissue Environment). The results of this phase are used to analyze how the depolarization patterns behave according to the granularity degree set for the gray zones.

Keywords**:** arrhythmia, virtual customized model, cardiac electrophysiology, gray zones, myocardium heterogeneities

1. Introduction

Coronary artery disease, characterized by blockages in the coronary arteries, frequently leads to myocardial ischemia: an interruption of the blood flow that supplies the myocytes causing tissue damage known as an infraction.
Infarcted myocardial tissue is made of non-excitable dead cells, however, there may be areas that go through a healing phase consisting of tissue remodeling, which sometimes goes beyond the actual infarct and affects the adjacent myocardium. These areas end up having cells with different levels of fibrosis, creating viable and nonviable paths for the electric signal. This characteristic granted them their name: Gray Zones.

These areas are often responsible for creating and maintaining arrhythmias as they may form reentrant loops. In this case, the electrical potential re-polarizes a region of myocytes after their refractory period, therefore the propagating impulse never dies out after the activation and persists re-exciting the heart, causing fibrillation, the muscle to flutter uncoordinated. The heart cannot maintain an effective contraction resulting in cardiac arrest.
When a patient is in cardiac arrest the only way to stop it is through defibrillation, applying a shock with a direct current strong enough to depolarize a large portion of the muscle, stopping the fluttering and allowing the sinoatrial node to start a new cardiac cycle.
Since 1980 [1] implantable cardio-defibrillators have been used as primary prevention to improve the survival of these patients, which is especially low outside the hospital.
Currently, the global metric to select patients for receiving this implant is based on the LVEF [2], which represents the percentage of blood that leaves the Left Ventricle (LV) in each contraction. In a healthy individual, this value is around 60%. If it remains below 35%, after three months of optimized medical treatment, the patient is eligible to receive an ICD [3][4].

However this metric is too generic, there is no guarantee that the patient will ever need defibrillation, resulting in unnecessary invasive procedures, and increasing the risk to the individual due to infection or even device malfunctions.
Several studies [5] show that two-thirds of SCD victims had an LVEF larger than 35%, therefore, were considered at low risk of suffering SCD and excluded by this metric.
Parallel customized models mimic the patient's myocardium, allowing for electrophysiological simulations to signal if there is a chance of the patient suffering from a fatal arrhythmia that can be prevented with an ICD.
To mimic the cardiac tissue depolarization wave, we need electrophysiological models that describe how the electricity flows through the heart while controlling muscle contraction. We developed and used an interface to generate such models from Late gadolinium enhancement (LGE) Magnetic Resonance Imaging (MRI) data sets; its main functionalities are reported in previous publications [6][7].

This paper presents the experiment of adding granularity to the gray zones identified in a patient-customized computational Left Ventricle model. Since our work is focused on creating an interface to manage all the stages of the model development, the methods are reported in pairs with the interface tools used in this stage of the pipeline.
It is reported how the scarred tissue identification is processed and how the conductivity values for each zone are computed.
The simulations run to compare how the depolarization patterns change by adding more levels to the gray zones are performed using the cardiac simulation software CHASTE.

2. Methods

A three-dimensional left ventricle model is built from an anonymized cardiac magnetic resonance data set.

This process involves translating two-dimensional images of the heart's short-axis plane where the left ventricle walls are visible, into a three-dimensional mesh that mimics the myocardium. Figure 1 shows one image taken from the dataset, with the left-ventricle myocardium borders countered.

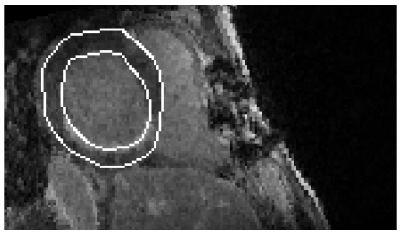

Fig. 1: Example of an image from the MRI dataset showing the heart's short axis plane with the left ventricle myocardium borders highlighted in white.

The myocardium is segmented in every image until the entire ventricle can be built from these slices. In each one, scarred tissue can be identified by applying segmentation methods previously validated for this end. Any slice can contain up to three types of tissue: Healthy (H), Scar (S), and Gray Zone (GZ).

For the work reported in this paper, the segmentation method applied is the 2-6 SD (Standard Deviation), which gives us two thresholds:

- Th_{GZ} = H tissue mean intensity + 2 SD;
- Th_S = H tissue mean intensity + 6 SD.

Following the scale in Figure 2, we can see how the myocardium is split into three groups, regarding the pixel's signal intensity:

- H, pixels with intensities below the Th_{GZ};
- GZ, pixels with intensity between Th_{GZ} and Th_S;
- S, pixels with intensities equal to and above Th_S.

Since we normalize the images, the intensity values can go from 0 seen as black to 1 seen as white. The higher (whiter) the value the more severe the damage.

The conductivity values for the whole GZ are set by applying an approach used in [8] and [9], where the transversal conductivity in the gray sections is set to 10% of the healthy one. This is a consequence of the re-modulation of myocytes at the scar borders that go through after infarction, in which the lateral gap junctions are affected.

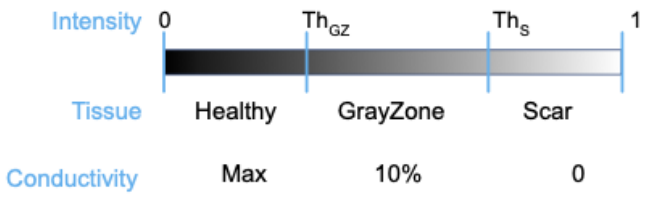

Fig. 2: Scale that illustrates how the pixels are defined according to their intensity. Th_{GZ} is the threshold for the GZ and Th_S the threshold for S. The conductivity for the transversal and normal directions in the GZ are set for 10% of the value set for H. The pixels that fall in the S area are set to 0 for every direction.

Figure 3 shows the result of this process for the same slice as Figure 1. The three tissue states are visible, the S and GZ are highlighted in red and Green respectively while the H tissue is the non-highlighted area left inside the outlined myocardium borders.

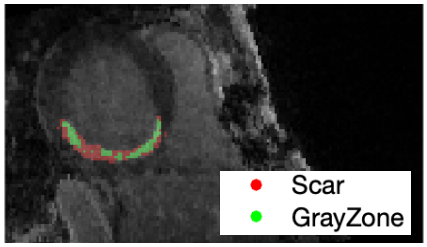

Fig. 3: Example of an image from the MRI dataset showing the heart's short-axis plane. The left ventricle myocardium borders are outlined in white and the tissue areas identified with the 2-6 SD method, S and GZ are highlighted in red and green respectively.

From these slices, the three-dimensional model is assembled. The rendering of the resulting structure that models the LV myocardium, is shown in figure 4. As in the 2D images, the tissue identified as S is displayed in red and the GZ in green.

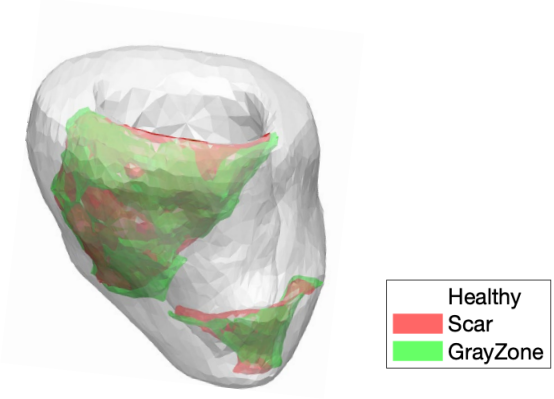

Fig. 4: 3D Rendering of the mesh built from the MRI dataset. Including the different tissues identified with the 2-6 SD method. S is represented in red green and GZ in green.

After the quantitative computation of the three main tissue statuses H, GZ, and S, a qualitative assessment is done to add sublevels to the GZ. These have different degrees of damage and therefore will be set to have different conductivities. A third threshold Th_{GZ2} is set to fall between and equally distanced from the two previously computed thresholds. The first threshold that marks the end of the H and the start of the GZ levels is named Th_{GZ1} from this point and while new levels may be added.

The scale in Figure 5 illustrates the new division of tissues according to pixel intensity. The conductivity for each GZ level increases by 10% the closer it is to the H tissue values. If another threshold is added, resulting in three levels for the GZ, the transversal and normal conductivity in the GZ_1 would be set to 30% of the H. GZ_2 would be 20% and GZ_3 10%.

Fig. 5: Scale that illustrates how the pixels are defined according to their intensity. Th_{GZ1} is the threshold for level 1 of the GZ, Th_{GZ2} for level 2 and Th_S the threshold for S. The conductivity for the transversal and normal directions in the GZ level 2 are set for 10% of the value set for H. In the GZ level 1, these are set for 20% of the value set for H. The pixels that fall in the S area are set to 0 for every direction.

Following this process, a second level was added to the GZ. The resulting three non-healthy tissues are mapped in the short-axis image of Figure 6. S is represented by red, GZ 1, composed of pixels with intensities closer to the ones in H, by blue, and GZ 2 by green.

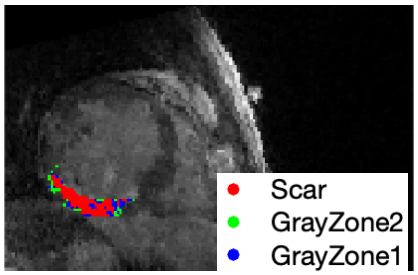

Fig. 6: 2D slice from the MRI dataset showing the heart's short axis plane with the S area marked in red and the two levels of GZ differentiated by green and blue.

The rendering of the resulting model is shown in Figure 7. As in the 2D image, the tissue identified as S is displayed in red, the GZ level 1 in blue and level 2 in green.

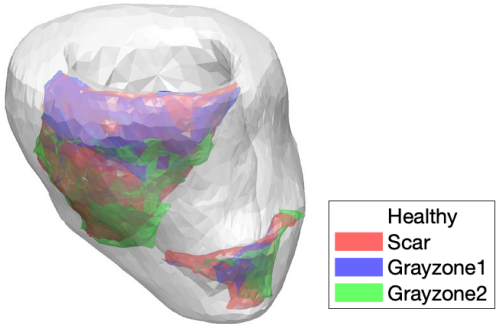

Fig. 7: 3D Rendering of the mesh built from the MRI dataset. Including the different tissues identified with the 2-6 SD method and the two grayzone levels. S is represented in red green and GZ 1in blue and GZ level 2 in green.

3. Results

Applying the described methods to the given dataset creates two left-ventricles with different tissue category distributions. Table 1 shows the volumes and percentages of tissue set to belong to each H, S, and GZ level in both scenarios.

Table 1: Volumes and percentages of each defined tissue resulted from each scenario.

		Volumes cm^3					Percentage			
Scenario	Gray zones	Total	H	S	GZ		H	S	GZ	
1	1	154.50	131.50	14.11	8.88		85.12%	9.13%	5.75%	
2	2	154.50	131.50	14.11	1| 5.68	2| 3.65	85.12%	9.13%	1| 2.87	2| 2.88%

An electrophysiological simulation was performed for each scenario using the same base settings. The LuoRudy Backward Euler ionic model for the monodomain was applied and the conductivities for the healthy tissue were adapted from the values reported in [10]. Since the goal was to mimic the left ventricle depolarization, which starts from the lowest part of the ventricle and goes up the walls until the base, a two-millisecond-long stimulus is administered in the apex.

Taking into account that the depolarization of the ventricles takes up to 120ms in a healthy heart and we are including a considerable percentage of non-healthy tissue, the simulation's duration was set to 200 ms.

The conductivities used for each tissue category in the first scenario simulation are presented in Table 2 and the ones for the second scenario in Table 3.

Table 2: Intracellular conductivities set for each tissue category in the first scenario simulation.

	Intracellular conductivities (mS/cm)	
Tissue category	Longitudinal	Transversal/Normal
Healthy	4.69	2.14
GrayZone	4.69	0.214
Scar	0	0

Table 3: Intracellular conductivities set for each tissue in the second scenario simulation.

	Intracellular conductivities (mS/cm)	
Tissue category	Longitudinal	Transversal/Normal
Healthy	4.69	2.14
GrayZone 1	4.69	0.428
GrayZone 2	4.69	0.214
Scar	0	0

The simulations results of both scenarios were then compared to assess the impact of the tissue categorization.

The 100 ms frame of the result depolarization maps for the simulated scenario 1 is presented in Figure 7 and the one for scenario 2 in Figure 8.

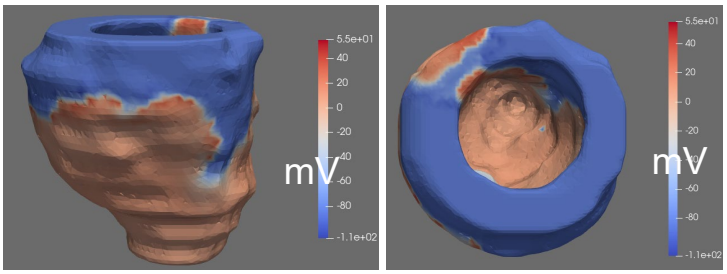

Fig. 7: Depolarization map at 100 ms for scenario 1, considering only one grayzone level. The view on the left is taken from the side and on the right is the view from the top of the left-ventricle base.

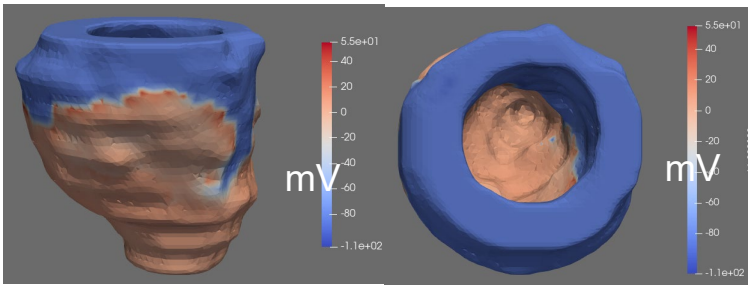

Fig. 8: Depolarization map at 100 ms for scenario 2, considering only two grayzone levels. The view on the left is taken from the side and on the right is the view from the top of the left-ventricle base.

The depolarization maps in Figures 7 and 8 show that the electric signal moves differently with the change of the grayzone granularity. In the top view, maps on the right, it is visible that the signal actually started to depolarize the base sooner when only one level was considered.

Table 4 summarizes the percentage of depolarized myocardium at four timesteps.

Table 4: Percentage of depolarized myocardium in the two simulated scenarios at specific timesteps.

		Timestep (ms)			
Scenario	Grayzone level	50	100	150	200
1	1	23.59%	54.84%	78.75%	56.28%
2	2	22.82%	50.65%	79.00%	56.90%
Difference of the % of depolarized tissue in scenario 2 compared to 1		-0.78%	-4.19%	+0.25%	+0.62%

From the first to the second scenarios, when the second Grayzone level is added, 2.87% of the myocardium gets s a 10% increase in the transversal and normal conductivities. From the last row of Table 4, we can see that this small difference caused a significant reduction in the quantity of myocardium that was depolarized up until the 150 ms mark and then an increase at the 200 ms mark.

4. Conclusions

This process had the purpose of evaluating the impact that the grayzones computation have on the heart models we are building.

In this experiment, even though the transversal and normal conductivities in the grayzones had values that a were at most 20% of the longitudinal conductivity, the depolarization wave propagation dynamic was highly affected. The results add to the premise that setting conductivity values for each tissue category is a big challenge, even though there are reported values from in vitro experiments and for healthy ventricles, it is possible to evaluate the resulting conductivity metrics, when working with the heterogenous tissue this is not the case, since the cardiac cycle won't obey standard timings.

References

[1] Marc W. Deyell, MD, FRCPC, Stanley Tung, MD, Andrew Ignaszewski, MD, F. (2010). The implantable cardioverter-defibrillator: From Mirowski to its current use. *BC Medical Journal*, *52*(5), 248.

[2] Goldberger, J. J., Cain, M. E., Hohnloser, S. H., Kadish, A. H., Knight, B. P., Lauer, M. S., Maron, B. J., Page, R. L., Passman, R. S., Siscovick, D., Stevenson, W. G., & Zipes, D. P. (2008). American Heart Association/American College of Cardiology Foundation/Heart Rhythm Society scientific statement on noninvasive risk stratification techniques for identifying patients at risk for sudden cardiac death: A scientific statement from the America. *Circulation*, *118*(14), 1497–1518. https://doi.org/10.1161/CIRCULATIONAHA.107.189375

[3] Disertori, M., Rigoni, M., Pace, N., Casolo, G., Masè, M., Gonzini, L., Lucci, D., Nollo, G., & Ravelli, F. (2016). Myocardial Fibrosis Assessment by LGE Is a Powerful Predictor of Ventricular Tachyarrhythmias in Ischemic and Nonischemic LV Dysfunction. JACC: Cardiovascular Imaging, 9(9), 1046–1055. https://doi.org/10.1016/j.jcmg.2016.01.033

[4] Goldberger, Z., & Lampert, R. (2006). Implantable Cardioverter-Defibrillators. *JAMA*, *295*(7), 809. https://doi.org/10.1001/jama.295.7.809

[5] Exner, D. v. (2009). Implantable cardioverter defibrillator therapy for patients with less severe left ventricular dysfunction. *Current Opinion in Cardiology*, *24*(1), 61–67. https://doi.org/10.1097/HCO.0b013e32831c4cc5

[6] Narciso, M., Ferreira, A., & Vieira, P. (2020). Incorporating tissue heterogeneities into 3D computational heart models. In P. Maria Manuela Cruz-Cunha, Polytechnic Institute of Cávado and Ave, Portugal Ricardo Martinho, Polytechnic Institute of Leiria, P. Rui Rijo, Polytechnic Institute of Leiria, P. Nuno Mateus-Coelho, Instituto Politécnico de Gestão e Tecnologia, & P. Dulce Domingos, LASIGE, Faculdade de Ciências, Universidade de Lisboa, Portugal Emanuel Peres, University of Trás-os-Montes e Alto Douro (Eds.), *Book of industry papers, poster papers and abstracts of the CENTERIS 2020* (pp. 225–232).

[7] Narciso, M., Sousa, A., Crivellaro, F., Valente de Almeida, R., Ferreira, A., & Vieira, P. (2020). Left Ventricle Computational Model based on Patients Three-dimensional MRI. *Proceedings of the 13th International Joint Conference on Biomedical Engineering Systems and Technologies*, 156–163. https://doi.org/10.5220/0008961601560163

[8] Costa, C. M., Plank, G., Rinaldi, C. A., Niederer, S. A., & Bishop, M. J. (2018). Modeling the electrophysiological properties of the infarct border zone. In Frontiers in Physiology (Vol. 9, Issue APR). Frontiers Media S.A. https://doi.org/10.3389/fphys.2018.00356

[9] Deng, D., Arevalo, H., Pashakhanloo, F., Prakosa, A., Ashikaga, H., McVeigh, E., Halperin, H., & Trayanova, N. (2015). Accuracy of prediction of infarct-related arrhythmic circuits from image-based models reconstructed from low and high resolution MRI. *Frontiers in Physiology*, *0*(OCT), 282. https://doi.org/10.3389/FPHYS.2015.00282

[10] Sachse FB, Moreno AP, Seemann G, Abildskov JA. A Model of Electrical Conduction in Cardiac Tissue Including Fibroblasts *Annals of Biomedical Engineering*, May 2009, volume 37, *number 5*, 874–89.